Enhanced Bose–Einstein condensation and kinetic energy of liquid ^{4}He near a free surface

2004 J. Phys.: Condens. Matter 16 4391

(http://iopscience.iop.org/0953-8984/16/24/020)

INSTITUTE OF PHYSICS PUBLISHING JOURNAL OF PHYSICS: CONDENSED MATTER

J. Phys.: Condens. Matter **16** (2004) 4391–4402 PII: S0953-8984(04)73593-6

Enhanced Bose–Einstein condensation and kinetic energy of liquid ^{4}He near a free surface

J V Pearce[1,7], S O Diallo[2], H R Glyde[2], R T Azuah[3,4], T Arnold[5] and J Z Larese[5,6]

[1] Institute Laue-Langevin, 6 Rue J Horowitz, BP156, Grenoble 38042, France
[2] Department of Physics and Astronomy, University of Delaware, Newark, DE 19716-2570, USA
[3] Department of Materials Science and Engineering, University of Maryland, College Park, MD 20742-2115, USA
[4] NIST Center for Neutron Research, National Institute of Standards and Technology, Gaithersberg, MD 20988-8562, USA
[5] Oak Ridge National Laboratory, PO Box 2008, Oak Ridge, TN 37831, USA
[6] Department of Chemistry, 319 Buehler Hall, University of Tennessee, Knoxville, TN 37996-1600, USA

E-mail: pearce@ill.fr

Received 16 December 2003
Published 4 June 2004
Online at stacks.iop.org/JPhysCM/16/4391
doi:10.1088/0953-8984/16/24/020

Abstract

We present neutron scattering measurements of Bose–Einstein condensation (BEC) in liquid ^{4}He adsorbed in thick layers on an MgO substrate to study whether the condensate fraction, n_0, is increased near a free surface of liquid ^{4}He. The data show that there is definitely a condensate in the layers adsorbed on the substrate with a condensate fraction comparable to that of bulk liquid ^{4}He. Two methods of analysis are employed to cross-check the results. The data indicate that the condensate fraction increases significantly when the number of adsorbed layers is reduced. This effect is independent of the analysis technique used. In addition, a significant increase in the kinetic energy of the ^{4}He atoms is observed when the number of adsorbed layers is reduced.

1. Introduction

The idea of using neutrons to measure the condensate fraction of liquid ^{4}He was originally proposed by Miller *et al* [1] and Hohenberg and Platzman [2]. Essentially, in high momentum transfer neutron scattering measurements, the energy transfer E is Doppler broadened by the momentum distribution of the atoms in the liquid, $n(\mathbf{k})$. If there is a condensate present, the fraction of atoms with zero momentum, n_0, contributes an unbroadened peak to the dynamic structure factor, $S(Q, E)$. This peak appears in $S(Q, E)$ at $E = E_R$, where $E_R = \hbar Q^2/2M$ is

[7] Author to whom any correspondence should be addressed.

the free, stationary atom recoil frequency and M is the atomic mass. The atoms struck by the neutrons recoil. If the interaction of the recoiling atoms with their neighbours is neglected, n_0 can be extracted directly from $S(Q, E)$.

Modern measurements show conclusively that there are phonon–roton excitations, a Bose–Einstein condensate, and a finite superfluid fraction present in superfluid ^{4}He and that all these phenomena gradually become less significant as the temperature is increased, until they all disappear at exactly the same temperature T_λ. For bulk liquid ^{4}He, $T_\lambda = 2.177$ K.

When liquid ^{4}He is confined in porous media, the transition temperature T_λ is suppressed below its bulk value, and the critical exponent describing the temperature dependence of the superfluid fraction $\rho_S(T)$ is modified from its bulk value (see, e.g. [3]). As a general rule, the severity of these effects becomes greater as the degree of confinement increases. Inelastic neutron scattering measurements of the elementary excitations of liquid ^{4}He show that there is a well defined two-dimensional layer excitation associated with confining media such as xerogel and Vycor. These excitations propagate in the liquid layers close to the medium walls [4–6]. It has recently been demonstrated that well defined phonon–roton excitations exist above T_c in Vycor and Geltech [5, 6]. One explanation for this is that there is a localized condensate above T_c confined to isolated regions across a finite volume [7]. Long range phase coherence is thereby destroyed, and the effect of localized BEC can be studied using this type of system.

In this paper, we present direct measurements of the condensate fraction of liquid ^{4}He adsorbed on an MgO substrate, for a series of different layer coverages. The aim is to determine whether the reduced dimensionality of this system has a 'localizing' effect on the measured condensate fraction, and whether the increased proportion of atoms close to a free surface gives rise to any altered behaviour. This is achieved using high energy inelastic neutron scattering techniques. Such measurements are very difficult to achieve with this type of system, because to obtain the necessary two-dimensional system less than 1 cm^3 of liquid ^{4}He must be adsorbed on the MgO particles. This means that there is a limited number of helium scattering centres in the sample. Background subtractions from the empty cell and MgO are also necessary which further deteriorates the quality of the observed signal.

Because of the reduced statistical quality of the data in comparison with conventional bulk helium measurements, two analyses are described in this paper. The first analysis involves a direct extraction of the condensate fraction n_0 from the experimental data; the second involves a direct extraction of the ^{4}He kinetic energy $\langle K \rangle$, from which n_0 can be obtained indirectly. The experimental procedure is described in section 2. The data analysis is presented in section 3, and a discussion is offered in section 4. We note that the quantity of liquid ^{4}He adsorbed on the flat surface offered by the MgO is measured in this paper in terms of the number of layers. The quantity thus given is nominal and represents an amount of liquid ^{4}He *equivalent* to the number of layers; the layer growth behaviour of this system is not well understood at present.

2. Experimental details

The substrate on which the liquid ^{4}He was adsorbed was MgO, chosen for its regular surface and its regular distribution of particle size ($\sim$1000 Å) [8, 9]. The MgO particles have a surface area of $\sim$10 m^2 g^{-1}. After extended baking at 950 °C for several days, the MgO powder was placed in a cylindrical Al sample cell of diameter 43 mm and height 58 mm. The sample cell was aligned with its vertical axis lying horizontal relative to the incoming beam in transmission geometry. The cell was attached to a ^{3}He sorption cryostat. A germanium resistance temperature sensor mounted at one end of the cell provided sample temperature readings. The temperature was controlled with a heater element attached to the cell and controlled by a Neocera temperature controller giving temperature stability to within 0.01 K.

The experiment was performed using the MARI time-of-flight (TOF) chopper spectrometer at the ISIS spallation source at the Rutherford Appleton Laboratory in the United Kingdom. MARI is a direct geometry chopper spectrometer which uses the TOF method, in which the time of arrival of a neutron in the detector, measured from when the neutrons leave the moderator, determines its energy loss or gain after scattering within the sample. The momentum transfer depends on both the TOF of the neutron and its scattering angle. More than 900 ^{3}He gas detectors provide a coverage of scattering angles between 3° and 135° in steps of 0.43°. A large range of momentum and energy transfer can therefore be observed simultaneously. For this measurement, an incident energy of 750 meV was selected using the low resolution Fermi chopper, giving an energy resolution of approximately 25 meV. For MARI in this configuration, the energy resolution function was approximated by a Gaussian function, whose width was calculated as a function of Q and E by analytical means. In this configuration wavevectors $Q < 30$ Å^{-1} and energies $E < 700$ meV were accessible.

Before condensing any helium in the cell, the background was measured from the sample can and MgO powder, and a second background was taken at a temperature of $T = 0.6$ K after adsorbing two solid layers onto the substrate. Measurements were then taken at two temperatures above and below T_λ at fillings of 12 liquid layers ($T = 0.6$ and 2.3 K), 22 liquid layers ($T = 0.6$ and 2.3 K), and 50 liquid layers ($T = 0.6$ and 3.5 K; at this filling the temperature could not be controlled reliably at 2.3 K). A custom-built, highly accurate computer-controlled gas handling panel was used to administer well defined doses of ^{4}He to the cell (see [29] for a more detailed description of this system). Thus the amount of ^{4}He condensed was known accurately. During the experiment, an estimate of the number of layers of liquid ^{4}He adsorbed was obtained by calculation from the known dimensions, density, amount, and packing fraction of the MgO. This value was measured more accurately after the experiment by performing a careful adsorption isotherm with the experimental set-up *in situ*. From the adsorption isotherm, the filling corresponding to completion of the first layer can be clearly identified, providing a calibration between the amount of ^{4}He adsorbed and the number of layers. Agreement between the calculated and measured amounts was close. In this paper the quoted layer coverages are the measured ones.

Standard procedures were employed to convert the raw neutron scattering data from TOF and intensity to E and the dynamic structure factor $S(Q, E)$. An excellent summary of these conversions has been given by Andersen *et al* [10]. Figure 1 presents the data converted to energy transfer and $S(Q, E)$. The data was then converted to the 'y scaling' energy transfer variable $y = (E - E_R)/v_R$, so that $J(Q, y) = v_R S(Q, E)$, where $E_R = \hbar Q^2/2m$ and $v_R = \hbar Q/m$ are the free atom recoil frequency and velocity, respectively. The results were studied in detail for $25.0 \leqslant Q \leqslant 28.5$ Å^{-1} in steps of 0.5 Å^{-1}, where final state (FS) broadening effects arising from interactions of the ^{4}He atoms after the recoil are small and $J(Q, y)$ varies slowly with Q.

3. Results

Figure 2 shows the dynamic structure factor, $S(Q, E)$, of liquid ^{4}He adsorbed on the MgO surface expressed as $J(Q, y)$. The statistical precision is considerably lower than that of previous measurements of bulk liquid ^{4}He, because much less sample (and therefore fewer scattering centres) can be placed in the beam.

The width of $J(Q, y)$ is approximately proportional to the mean square atomic momentum along Q, $\langle k_Q^2 \rangle$. The atomic kinetic energy is given by $\langle K \rangle = (3\hbar^2/2m)\langle k_Q^2 \rangle$. The contribution to $J(Q, y)$ arising from the condensate manifests itself chiefly as extra intensity at $y = 0$ giving a higher peak in $J(Q, y)$ in superfluid ^{4}He. The condensate term $n_0 R(Q, y)$ in $J(Q, y)$, where

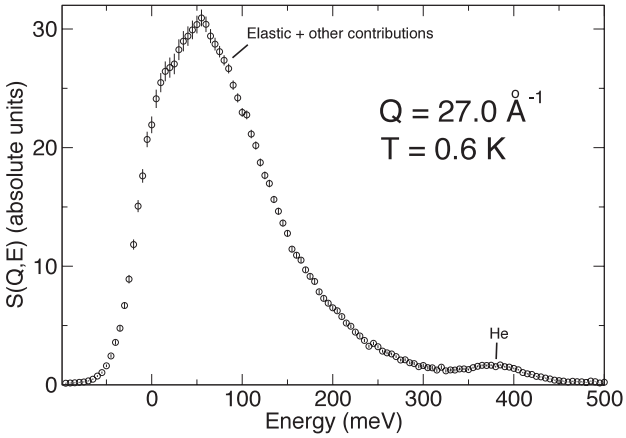

Figure 1. Typical raw $S(Q, E)$ taken on MARI at a wavevector of 27 Å^{-1}, $T = 0.6$ K (50 layers). The limited amount of liquid helium in the beam, together with the large elastic scattering from the MgO and other contributions, means that the signal to background ratio is very low.

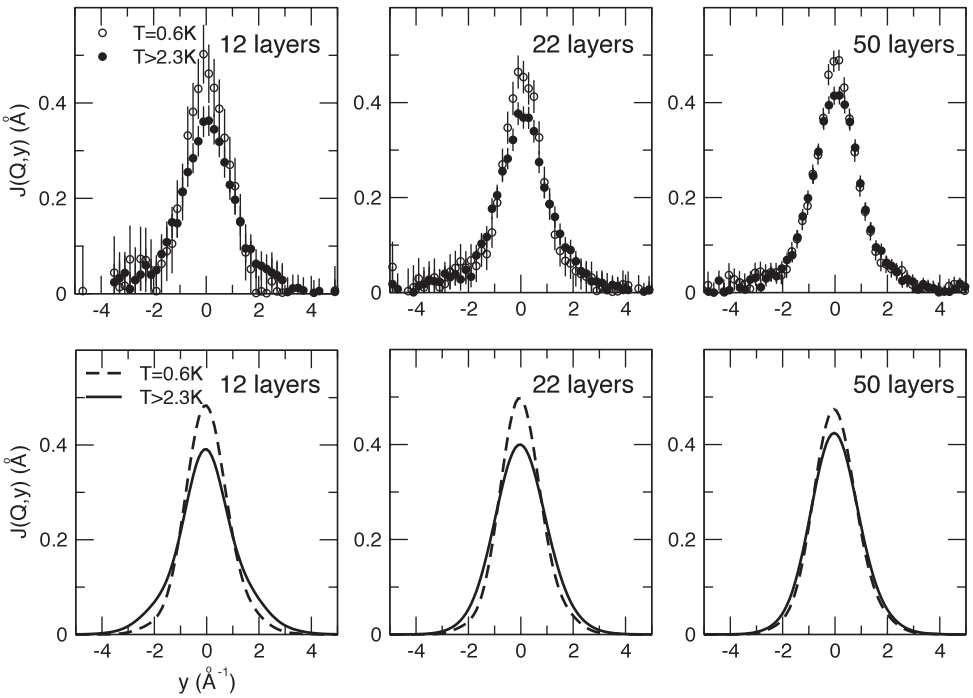

Figure 2. The observed $J(Q, y)$ at a wavevector of 27 Å^{-1} at 12 layers (left), 22 layers (middle), and 50 layers (right). The top row represents the experimental data, and the bottom row represents fits to the data as described in the text.

$R(Q, y)$ is the FS broadening function, also introduces a left–right asymmetry in the superfluid data.

For the purpose of analysis, $J(Q, y)$ is expressed as a convolution of the impulse approximation (IA) to $J(Q, y)$, $J_{\mathrm{IA}}(y)$, and the FS broadening function, $R(Q, y)$, that is,

$J(Q, y) = J_{\mathrm{IA}}(y) \otimes R(Q, y)$. The IA is expressed as

$$J_{\mathrm{IA}}(y) = \int \mathrm{d}\mathbf{k}\, n(\mathbf{k})\delta(y - k_Q) \tag{1}$$

where $k_Q = \mathbf{k} \cdot \hat{\mathbf{Q}}$ and $n(\mathbf{k})$ is the atomic momentum distribution. The observed data is also convoluted with the resolution function $I(y)$ so that $J_{\mathrm{obs}}(Q, y) = J(Q, y) \otimes I(y)$. The momentum distribution in $J_{\mathrm{IA}}(y)$ is represented as

$$n(\mathbf{k}) = n_0[\delta(\mathbf{k}) + f(\mathbf{k})] + A_1 n^*(\mathbf{k}). \tag{2}$$

Here $n_0\delta(\mathbf{k})$ is the condensate contribution. A_1 is a constant and $n^*(\mathbf{k})$ is the momentum distribution of atoms above the condensate ($k \neq 0$), normalized to unity[8]. Normalizing $n(\mathbf{k})$ gives $\int \mathrm{d}\mathbf{k}\, n(\mathbf{k}) = n_0\left[1 + I_f\right] + A_1 = 1$ where $I_f = \int \mathrm{d}\mathbf{k}\, f(\mathbf{k}) \approx 0.25$. The term $n_0 f(\mathbf{k})$ arises from a coupling between the single-particle and density excitations via the condensate and is very sharply peaked at $k = 0$. It is defined as

$$n_0 f(\mathbf{k}) = \left[\frac{n_0 mc}{2\hbar\left(2\pi^3 n\right)}\frac{1}{|\mathbf{k}|}\coth\left(\frac{c\hbar|\mathbf{k}|}{2k_{\mathrm{B}}T}\right)\right] \mathrm{e}^{-k^2/(2k_c^2)}. \tag{5}$$

The term in square brackets is the derived expression valid at low k, where $n = N/V$ is the liquid density and c is the speed of sound in liquid helium. This expression has been multiplied by a Gaussian to cut off $f(\mathbf{k})$ at higher k because $f(\mathbf{k})$ must disappear before the end of the phonon region, $k = 0.7$ Å^{-1}. The quality of the current data is only sufficient to extract one parameter. Therefore we elect to perform two different analyses for the purpose of cross-checking the results. The first analysis is to extract the condensate fraction n_0 directly from $J(Q, y)$. The second analysis is to extract the ^{4}He kinetic energy $\langle K\rangle$ from $J(Q, y)$. A knowledge of the kinetic energy in the superfluid and normal phases allows extraction of n_0. The two analyses can then be compared.

3.1. Analysis I: direct extraction of n_0

To extract the condensate fraction, n_0, a function $J(Q, y) = J_{\mathrm{IA}}(y) \otimes R(Q, y)$ was fitted to the experimental $J(Q, y)$. This fitted function explicitly contains a contribution from the condensate, and has Gaussian, fourth cumulant, and sixth cumulant components. The components were set as follows. The values $k_c = 0.5$ Å^{-1}, $\alpha_2 = 0.884$ Å^{-2}, $\alpha_4 = 0.48$ Å^{-4}, and $\alpha_6 = 1.03$ Å^{-6}, which are concerned with the momentum distribution, and $\beta_3 = 0.098\,21$ Å^{-3}, $\beta_4 = 0$, $\beta_5 = 0.1002$ Å^{-5}, and $\beta_6 = 0.2232$ Å^{-6}, which are concerned with the FS effects, were all kept fixed at their bulk values obtained with the benchmark measurements

[8] The derivation of $n(\mathbf{k})$ can be summarized as follows. At high Q, the scattering time t and the distance travelled by the struck atom $s = (\hbar Q/M)t$ within the scattering time are short. This gives rise to a short-time expansion of $J(Q, s)$ and $J_{\mathrm{IA}}(s) = \langle \mathrm{e}^{-\mathrm{i}k_Q s}\rangle$ in powers of s:

$$J_{\mathrm{IA}}(s) = \exp\left[-\frac{\bar{\alpha}_2 s^2}{2!} + \frac{\bar{\alpha}_4 s^4}{4!} - \frac{\bar{\alpha}_6 s^6}{6!} + \cdots\right] \tag{3}$$

where $\bar{\alpha}_2 = \langle k_Q^2\rangle$, $\bar{\alpha}_4 = \langle k_Q^4\rangle - 3\langle k_Q^2\rangle^2$, and $\bar{\alpha}_6 = \langle k_Q^6\rangle - 15\langle k_Q^4\rangle\langle k_Q^2\rangle + 30\langle k_Q^2\rangle^3$ are the cumulants of the momentum distribution $n(k_Q)$. An expansion of $R(Q, s)$ can be performed in a similar way:

$$R(Q, s) = \exp\left[\frac{\mathrm{i}\beta_3 s^3}{3!} + \frac{\beta_4 s^4}{4!} - \frac{\mathrm{i}\beta_5 s^5}{5!} - \frac{\beta_6 s^6}{6!} + \cdots\right] \tag{4}$$

where $\bar{\beta}_3 = \bar{a}_3/\lambda Q$, $\bar{\beta}_4 = \bar{a}_4/(\lambda Q)^2$, $\bar{\beta}_5 = \bar{a}_{52}/(\lambda Q)^3 + \bar{a}_{54}/\lambda Q$, and $\bar{\beta}_6 = \bar{a}_{62}/(\lambda Q)^4 + \bar{a}_{64}/(\lambda Q)^2$ and $\lambda = \hbar^2/M = 1.0443$ meV Å^2. Expressions for the $\bar{a}_n$ can be obtained from the moments of $J(Q, y)$ and results up to $\bar{a}_{64}$ have been derived [11, 12]. To summarize, $J_{\mathrm{IA}}(s)R(Q, s)$ has a total of eight parameters: n_0, $\bar{\alpha}_2$, $\bar{\alpha}_4$, and $\bar{\alpha}_6$, which determine $J_{\mathrm{IA}}(s)$, and $\bar{\beta}_3$, $\bar{\beta}_4$, $\bar{\beta}_5$, and $\bar{\beta}_6$, which determine the FS function $R(Q, s)$.

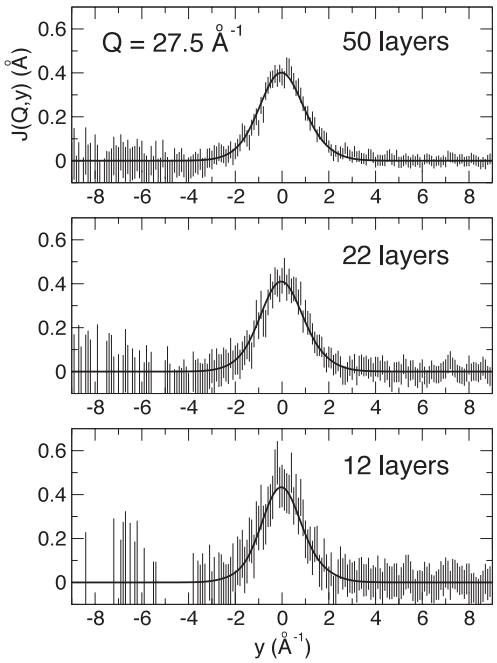

Figure 3. Representative fits to $J(Q, y)$ at a wavevector of 27.5 Å^{-1}, $T = 0.6$ K.

Table 1. Table showing the values of n_0 extracted directly from $J(Q, y)$, obtained at each filling.

Filling (layers)	n_0 (%)
12	13.466 ± 2.730
22	9.315 ± 1.752
50	6.882 ± 0.620

of Glyde *et al* [13]. Physically, $R(Q, y)$ depends on the short range interaction between pairs of atoms (specifically, it depends on the hard core of the pair potential [32]), and much less on the overall density. It is found to be the same in superfluid and normal liquid ^{4}He (differing densities), and in solid ^{4}He (much higher density). All indications are that $R(Q, y)$ will be the same in a thick film, as used here, as in the bulk even though it is likely that the density is less than the bulk density near the film surface.

The weight of $J_{\mathrm{IA}}(Q, y)$ was kept fixed at unity. The parameter n_0 was allowed to vary and determined by a least squares fit to the data. This approach offers a direct way of obtaining n_0. A typical fit of this function to the experimental data is shown by the solid curve in figure 3. The resulting variation of n_0 with Q at the three different fillings is presented in figure 5. A least squares fit of a straight line to the data, weighted by the error of the individual points, has been performed to find the mean n_0 for each filling. The results are presented in table 1 and figure 6, which clearly indicate that n_0 increases significantly as the number of layers decreases. This effect can be seen in figures 3 and 4.

We note that the values of $n_0(T)$ for a 50-layer coverage are approximately comparable to the accurate bulk values, and as the number of layers is reduced n_0 increases. We also note that this approach avoids the difficulties of the approach of Sears [14], where the kinetic energies above and below T_λ are compared to give n_0, and which is found to overestimate n_0 [13, 15]. This has been attributed by Azuah *et al* and Mayers *et al* [16] to the fact that fitting a function $J(Q, y)$ that does not contain a condensate to data that do contain a condensate underestimates

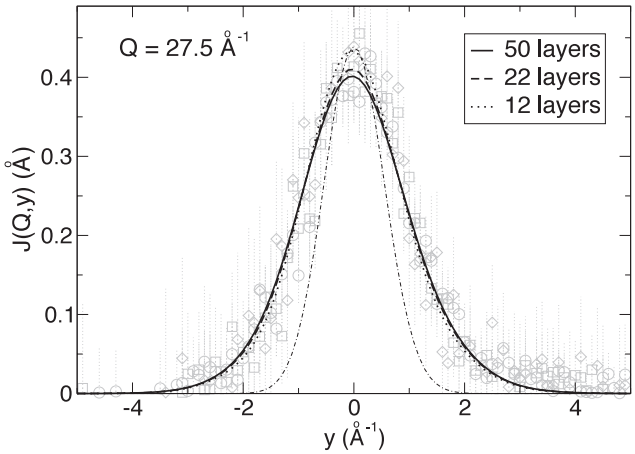

Figure 4. Fits and data at the three coverages, superimposed for clarity. $Q = 27.5$ Å^{-1}, $T = 0.6$ K. The thin dash–dotted curve represents the instrumental resolution function.

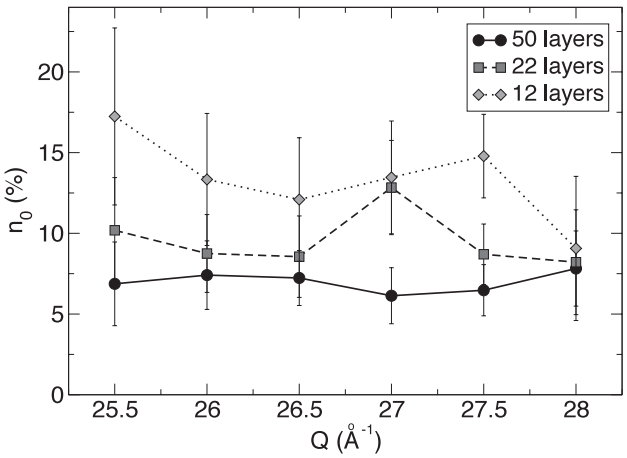

Figure 5. Q dependence of the condensate fraction n_0 at $T = 0.6$ K. The lines joining the points are for clarity. Dotted line, 12 layers; dashed line, 22 layers; solid line, 50 layers.

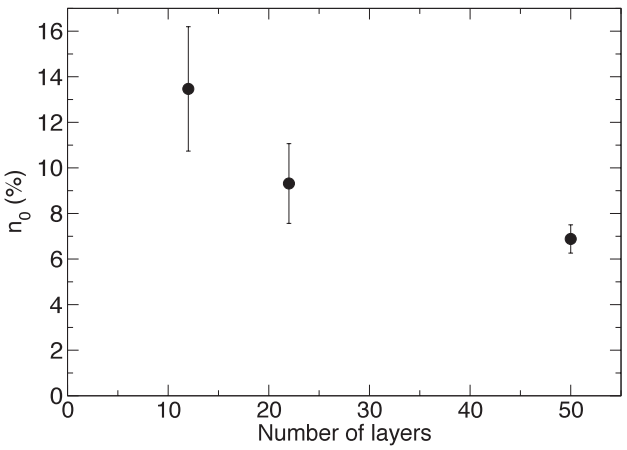

Figure 6. Condensate fraction, n_0, in ^{4}He adsorbed on MgO as a function of film thickness. There is a clear trend towards higher n_0 as the number of layers decreases.

$\langle K \rangle$. With that method, it follows that an underestimate of $\langle K \rangle$ gives an overestimate of n_0. We believe that a direct extraction of n_0 avoids this problem, although implicit in this technique is the assumption that the kinetic energy of helium atoms in this system is the same as that of

the bulk. This is because the quality of the data is not sufficiently high to allow fitting of both n_0 and the second moment α_2.

We remark that since the precise nature of the coverage dependence of the kinetic energy is not known, there is the possibility that it is invalid to use the bulk value of the kinetic energy, α_2. An inaccurate value of the kinetic energy will yield an inaccurate value of n_0. However, trial fits with varying α_2 indicate that, although the extracted value of n_0 is affected, its variation with the number of layers remains qualitatively similar.

3.2. Analysis II: method of Sears

As the quality of the current data is only sufficient to extract one parameter from the fit, we attempt a second method, which is to extract the second moment, or width, of the data. To do this, we determined $n_0(T)$ from the second moment of $J(Q, y)$ following a method proposed originally by Sears [17, 14] and exemplified in [13]. In this scheme, $n_0(T)$ is determined from the second moment of $J(Q, y)$ which is $M_2 = \int \mathrm{d}y\, y^2 J(Q, y)$. The FS function $R(Q, y)$ is normalized to unity and its second moment is zero. Because of this, M_2 is the second moment of $J_{\mathrm{IA}}(y)$: $M_2 = \int \mathrm{d}y\, y^2 J_{\mathrm{IA}}(y)$. From (1): $M_2 = \langle k_Q^2 \rangle = \int \mathrm{d}\mathbf{k}\, k_Q^2 n(\mathbf{k})$. A key aspect of this method is that when there is a condensate present, the first two terms of (2), i.e. $n_0\delta(\mathbf{k})$ and $n_0 f(\mathbf{k})$, are so sharply peaked at $\mathbf{k} = 0$ that they do not contribute to the second moment $\langle k_Q^2 \rangle$. So from (2), $\int \mathrm{d}\mathbf{k}\, k_Q^2 n(k) = A_1 \int \mathrm{d}\mathbf{k}\, k_Q^2 n^*(\mathbf{k})$. We note that rather than calculating M_2, which is prone to large errors when fitting to statistically noisy data, we obtain it by fitting a function which contains it to the data as described below.

The important result of this is that the condensate does not make any contribution to the kinetic energy, $\langle K \rangle = \left(3\hbar^2/2m\right) \langle k_Q^2 \rangle$, and therefore $\langle K \rangle$ gets smaller as the condensate appears. The value of n_0 can be obtained by measuring the drop in kinetic energy. In the normal phase, $\langle k_Q^2 \rangle_N = \int \mathrm{d}\mathbf{k}\, k_Q^2 n_N(\mathbf{k})$ where $n_N(\mathbf{k})$ can be obtained from (2) by setting $n_0 = 0$ and $A_1 = 1$.

Bulk measurements indicate that $n_N(\mathbf{k})$ and $n^*(\mathbf{k})$ are the same [13]. This means that

$$\langle K \rangle / \langle K \rangle_N = \langle k_Q^2 \rangle / \langle k_Q^2 \rangle_N = A_1. \tag{6}$$

By combining this expression with the normalization expression for $n(\mathbf{k})$, $n_0 \left[1 + I_f\right] + A_1 = 1$, the condensate fraction n_0 can be expressed as a function of the change in kinetic energy between the superfluid ($\langle K \rangle$) and normal fluid ($\langle K \rangle_N$) states:

$$n_0 = \frac{1 - \langle K \rangle / \langle K \rangle_N}{1 + I_f} \tag{7}$$

where we recall that $I_f = 0.25$. As described in the previous analysis, the expression $J(Q, y) = J_{\mathrm{IA}}(y) \otimes R(Q, y)$ was fitted to the experimental $J(Q, y)$. As before, all parameters were kept fixed at their bulk values obtained with the benchmark measurements of Glyde *et al* [13] with the exception of the width α_2, which is related to the kinetic energy and is a free parameter in the fit. The weight was kept fixed at unity, and the function contains no contribution from the condensate. Having established the kinetic energy $\langle K \rangle$ above and below T_λ, the condensate fraction can be obtained using (7).

The Q dependence of the fitted parameter α_2 at low temperature (0.6 K) and high temperature (>2.3 K) are presented in figure 7. A value for n_0 was then obtained at each Q using the expression of Sears presented in (7). A least squares fit of a straight line to the data, weighted by the error of the individual points, has been performed to find the mean n_0 for each filling. The results are presented in table 2, which clearly indicates that n_0 increases significantly as the number of layers decreases, while the kinetic energy exhibits a high sensitivity to both the number of layers and the temperature.

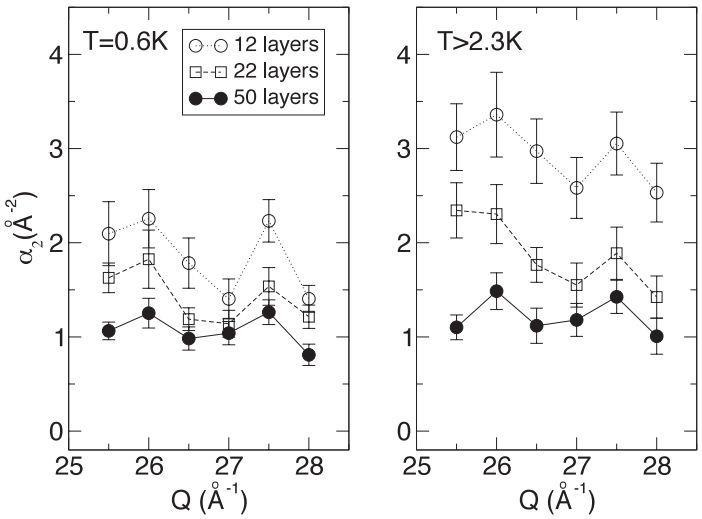

Figure 7. Q dependence of the fitted parameter α_2 at $T = 0.6$ K (left) and $T > 2.3$ K (right) (Sears method). The lines joining the points are for clarity.

Table 2. Table showing the values of n_0 for each filling, and the width of $J(Q, y)$ (kinetic energy) obtained in the superfluid and normal phase (Sears method).

Filling (layers)	n_0 (%)	$\langle K \rangle$ (K)	$\langle K \rangle_N$ (K)
12	32.80 ± 8.94	27.23 ± 2.56	46.15 ± 4.03
22	21.46 ± 4.51	21.02 ± 1.49	28.72 ± 2.25
50	10.54 ± 1.78	16.73 ± 1.05	19.27 ± 1.18

It is necessary at this point to make a few remarks about the method of Sears. There is a complication of the current data in that we already know that for higher T the increased vapour pressure gives rise to evaporation of a significant fraction of the sample, which means that the coverage drops by approximately 15%.

The volume of the sample cell and capillary line above the cell (the 'dead space') is approximately 75 cm^3. At very low temperature this is an effective volume of approximately 200 cm^3. That is, the amount of gas that occupies 75 cm^3 will occupy 200 cm^3 at room temperature. For a coverage of ten layers (6000 Torr in 81 cm^3 is 48 600 Torr cm^{-3}), the vapour pressure is approximately 30 Torr at 2.3 K. Therefore, the amount of gas in the dead space is $35.200 = 7000$ Torr cm^{-3}, which is around 15%.

If the kinetic energy is sensitive to the coverage, as indicated by the current data, a decreased coverage could lead to a higher indicated $\langle K \rangle$. Thus, from (7), n_0 would be overestimated. This 'error' in n_0 would be larger at lower coverages because the change in the coverage with temperature is proportionately larger at lower coverages.

Since the precise nature of the coverage dependence of $\langle K \rangle$ is not known, it is not possible to correct the current data for this effect with any kind of accuracy or precision, but we note its presence and that fact that order-of-magnitude calculations indicate an over-estimate of n_0 of approximately 15% for the measurement at 12 layers, and approximately 7.5% for the measurement at 22 layers.

Thus we find that $\langle K \rangle$ increases as the layer thickness is decreased, particularly in the normal phase. When these $\langle K \rangle$ values are used in the Sears method, greatly increased n_0 values are obtained for 12- and 22-layer films as shown in table 2. This is probably an overestimate of n_0 as discussed below.

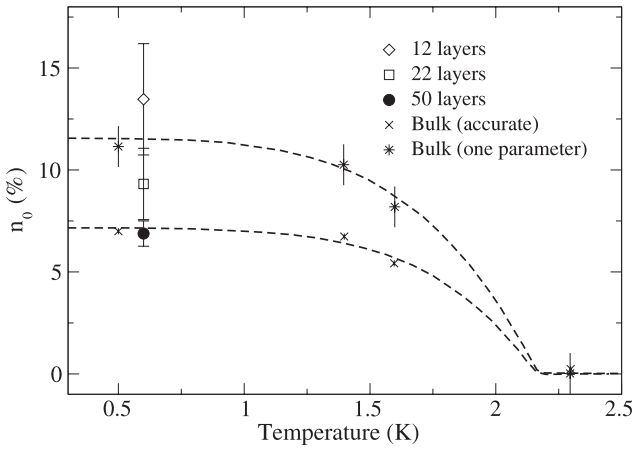

Figure 8. Temperature dependence of the condensate fraction obtained in previous measurements using the most accurate figures [13] for the bulk (crosses) and the one-parameter fitting method using the same data from that measurement (stars). The results from the current measurement (diamonds, squares, and circles) are overplotted. The value of n_0 at 50 layers is comparable to that of the bulk, but the lower fillings clearly appear to have a much larger condensate fraction.

4. Discussion

BEC is thought to play a major role in the superfluid behaviour of liquid ^{4}He. The small condensate fraction in bulk liquid ^{4}He has been shown to exist unambiguously using neutrons, and has been accurately measured to be $n_0 = 7.25 \pm 0.75\%$ [13]. BEC also exists in liquid ^{4}He in porous media such as Vycor. In the three-dimensional system there is phase coherence in the condensate over macroscopic length scales, supporting superflow across the whole fluid volume. In the two-dimensional system there can also be BEC but the coherence has a power law decay over length scales of a few atomic separations only [18]. There is therefore no long range phase coherence in BEC [19] or long range order in the two-dimensional system [20].

We have performed measurements on MARI which indicate that there is definitely a condensate in the layers of liquid ^{4}He adsorbed on the surface of MgO particles. Figure 8 shows the current values of n_0 at each filling in the context of previous measurements of the temperature dependence of n_0. Within error, the condensate fraction appears to increase as the number of layers is reduced. As n_0 is a sensitive function of pressure, the observed increase in n_0 may not be unreasonable.

The extracted condensate fraction n_0 is unexpectedly large, especially at lower fillings. It has already been demonstrated by Adams *et al* [21] that the density of liquid helium confined in porous Vycor glass is higher than that of the bulk, which should give rise to a lower condensate fraction on account of the increased interatomic interactions [22]. However, it may also be that as the number of layers is reduced, the pressure of the liquid within the layers is reduced. A reduction in the pressure (and therefore density) of the liquid means that the interatomic interactions become less influential, and give rise to a less suppressive effect on the formation of the condensate.

4.1. Enhancement of kinetic energy near a surface

This experiment clearly shows an increased kinetic energy of the helium atoms at lower coverages. This effect has been observed before in helium adsorbed on activated carbon fibres (ACFs) (see e.g. [23]).

The enhancement in thinner films is largest in the normal phase. Since it is assumed in the Sears method that all the difference in $\langle K \rangle$ between the superfluid and normal phase arises from n_0, this method will overestimate n_0 if the increase in $\langle K \rangle$ in the normal phase has other origins. The n_0 obtained using the $\langle K \rangle$ values is presented here solely for the purpose of demonstrating an alternative method of analysis.

It is clear, however, that in both the superfluid and normal phases fitting a function without a condensate to the data and allowing the width to vary freely yields a broadening of $J(Q, y)$ as the film gets thinner. This result is significant and appears to be independent of the function used to model the data. Thus the kinetic energy is significantly larger in thin films compared with the bulk. This is especially true in the normal phase.

4.2. Enhancement of BEC near a surface

Lewart *et al* [24] have calculated the condensate fraction in the low density region near a ^{4}He surface. Griffin and Stringari [25] have remarked that this calculated value is significantly larger than the value in bulk helium of approximately 10%. Subsequent calculations have been performed [26, 27] and predicted condensate fractions of up to 100% in similar systems, and at the surface of a dense liquid of bosons in a trap [30]. However, some of these results were found to be highly dependent on the choice of trial wavefunction.

The assertion of Griffin and Stringari has recently been convincingly supported by the path integral Monte Carlo simulations of Draeger and Ceperley, who simulated a finite-thickness helium slab [28]. This simulation consisted of a system of ^{4}He atoms, interacting pairwise with an accurate potential. They found that as one moves through the helium surface, the condensate fraction initially increases as the density decreases, as a result of the decreasing effect of helium–helium interactions. The condensate fraction reaches a maximum value of 93%. As the density decreases further, the condensate fraction begins to decrease, possibly due to interaction with ripplons at the surface of the slab. Experimental probes of a thin helium film adsorbed on a surface should therefore reveal an enhanced condensate fraction. This is borne out by our current measurements. We note also the definitive measurements of Wyatt [31] which provided experimental confirmation of the enhancement of the condensate fraction near a surface.

5. Conclusion

We have measured the inelastic neutron scattering spectrum of liquid ^{4}He adsorbed on MgO with coverages of 12, 22, and 50 layers in the superfluid and normal phases. We have presented two different analyses, with the aim of examining the condensate fraction and kinetic energy. The first analysis involves a direct extraction of the condensate fraction from the experimental $J(Q, y)$, and we report on the values obtained. The second analysis involves a direct extraction of the kinetic energy from the second moment of the experimental $J(Q, y)$, and an indirect extraction of the n_0 is reported but we do not place a strong emphasis on it. However, both methods agree qualitatively.

We find that this measurement offers compelling evidence for an enhanced Bose condensate in thin layers of superfluid ^{4}He. This result is independent of the method used to analyse the data. The dramatic increase in the value of n_0 is an interesting result but the poor statistical quality of the current data means that only qualitative conclusions can be made, and more measurements of this type are necessary before making any firm quantitative conclusions. This is partly due to the difficulty in adsorbing enough helium onto an MgO surface to give a sufficiently large amount of scattering on MARI. We believe that a porous glass such as MCM-41 would be a more suitable medium for a further measurement on MARI, because its much larger surface area per unit volume would facilitate the adsorption of much more helium.

On MARI, sufficient helium could be adsorbed onto the surface of the MCM-41 pores to allow a measurement of the condensate fraction of a layer one atom thick.

In summary, we find that there is definitely Bose–Einstein condensation in thin films adsorbed on MgO crystals. Within the precision of the current measurements, there appears to be a significantly larger condensate fraction at lower coverages, which is an exciting result, and is in agreement with modern theoretical predictions [25, 28]. In addition, we find that the kinetic energy of the helium atoms increases when the number of layers is reduced in both the superfluid and normal phases, an effect which has also been observed for a monolayer of liquid ^{4}He adsorbed on activated carbon fibre [23]. This effect appears more pronounced in the normal phase. There is much work to be done to better characterize and explain the interesting behaviour of liquid ^{4}He close to a free surface.

Acknowledgments

We would like to thank R B E Down for his assistance on the beamline and J W Taylor for technical assistance with the MARI spectrometer. This work was partially supported by the National Science Foundation under grant number DMR-0115663. JZL and TA gratefully acknowledge funding from the US Department of Energy under contract DE-AC05-00OR22725 at ORNL managed by UT-Battelle, LLC.

References

[1] Miller A, Pines D and Nozieres P 1962 *Phys. Rev.* **127** 1452
[2] Hohenberg P C and Platzman P M 1966 *Phys. Rev.* **152** 198
[3] Reppy J D 1992 *J. Low Temp. Phys.* **87** 205
[4] Fåk B, Plantevin O, Glyde H R and Mulders N 2000 *Phys. Rev. Lett.* **85** 3886
[5] Glyde H R, Plantevin O, Fåk B, Coddens G, Danielson P S and Schober H 2001 *Phys. Rev. Lett.* **84** 2646
[6] Plantevin O, Fåk B, Glyde H R, Mulders N, Bossy J, Coddens G and Schober H 2001 *Phys. Rev.* B **63** 224508
[7] Fisher D S, Fisher M P A and Huse D A 1991 *Phys. Rev.* B **43** 130
[8] Larese J Z and Kunnmann W *US Patent Specification* 6179897
[9] Freitag A and Larese J Z 2000 *Phys. Rev.* B **62** 8360
[10] Andersen K H, Scherm R, Stunault A, Fåk B, Godfrin H and Dianoux A J 1994 *J. Phys.: Condens. Matter* **6** 821
[11] Glyde H R 1994 *Phys. Rev.* B **50** 6726
[12] Sears V F 1984 *Phys. Rev.* B **30** 44
[13] Glyde H R, Azuah R T and Stirling W G 2000 *Phys. Rev.* B **62** 14337
[14] Sears V F 1983 *Phys. Rev.* B **28** 5109
[15] Azuah R T, Glyde H R, Scherm R, Mulders N and Fåk B 2003 *J. Low Temp. Phys.* **130** 557
[16] Mayers J, Albergamo F and Timms D 2000 *Physica* B **276** 811
[17] Sears V F, Svensson E C, Martel P and Woods A D B 1982 *Phys. Rev. Lett.* **49** 279
[18] Ceperley D M 1995 *Rev. Mod. Phys.* **67** 279
[19] Hohenberg P C 1967 *Phys. Rev.* **158** 383
[20] Mermin N D and Wagner H 1966 *Phys. Rev. Lett.* **22** 1133
[21] Adams E D, Uhlig K, Tang Y H and Haas G E 1984 *Phys. Rev. Lett.* **52** 2249
[22] Snow W M, Wang Y and Sokol P E 1992 *Europhys. Lett.* **19** 403
[23] Nemirovsky D, Moreh R, Andersen K H and Mayers J 1999 *J. Phys.: Condens. Matter* **11** 6653
[24] Lewart D S, Pandharipande V R and Pieper S C 1988 *Phys. Rev.* B **37** 4950
[25] Griffin A and Stringari S 1996 *Phys. Rev. Lett.* **76** 259
[26] Galli D E and Reatto L 1998 *J. Low Temp. Phys.* **113** 223
[27] Galli D E and Reatto L 2000 *J. Phys.: Condens. Matter* **12** 6009
[28] Draeger E W and Ceperley D M 2002 *Phys. Rev. Lett.* **89** 15301
[29] Mursic Z, Lee M Y M, Johnson D E and Larese J Z 1996 *Rev. Sci. Instrum.* **67** 1886
[30] DuBois J L and Glyde H R 2001 *Phys. Rev.* A **63** 023602
[31] Wyatt A F G 1998 *Nature* **391** 6662
[32] Silver R N 1988 *Phys. Rev.* B **38** 2283